Problems and Capabilities in the Assessment of Parametric Rolling

<u>Kostas J. Spyrou</u>, Ioannis Tigkas, G. Scanferla & N. Gavriilidis

National Technical University of Athens, Greece

ABSTRACT

A step-by-step evaluation of some current methods for the prediction of parametric rolling is presented. In parallel, a continuation method is implemented for the investigation of parametric rolling, highlighting the enhanced scope achieved by it. The boundary line that is formed by the folding of the curve representing the amplitude of parametric oscillations as function of the frequency ratio is discussed in detail. Several other technical issues are discussed.

KEYWORDS

Ship; stability; parametric roll; containership.

INTRODUCTION

Parametric rolling is nowadays perhaps the most popular topic of ship stability research (Neves 2006). Methods targeting its prediction range from simple formulae based on Mathieu-type dynamics; to numerical codes based on detailed ship hydrodynamics. However, the true capability of current methods to capturing quantitatively the critical features of the phenomenon (in deterministic as well as in probabilistic sense) is still an open issue. Comparisons based on time histories obtained by a few simulation runs against experimental results are unlikely to be an effective way for resolving this, due to the several design and operational factors that influence the parametric rolling behaviour of ships.

A systematic investigation that has set its focus on the prediction potential of parametric rolling by the various available methods is discussed in the current paper. The numerical technique of continuation of nonlinear dynamics is the main vehicle of this investigation. Continuation is known to be helpful for tracing efficiently the entire set of a system's stable and unstable responses, for detecting safety boundaries and

in general for predicting critical phenomena. One by-product therefore of the current work is, better understanding of the value of continuation for the study of parametric rolling. Some of the issues that have been investigated are: a) the nature of the boundary lines that confine the principal region of parametric roll oscillations and also the dependence of the characteristics of the latter upon various parameters; b) the accuracy of available analytical formulae in reflecting the dynamics even within the context of a simple nonlinear Mathieu-type model of ship rolling; c) the influence on the boundaries of a non-harmonic variation $GZ(\varphi; t)$ exhibited by a ship due wave passage; and d) the effect of couplings due to pitch and heave in head seas.

REVIEW OF ANALYTICAL FORMULAE

In the ITTC (2005) guideline of parametric rolling expressions are based on the following model:

$$\ddot{\phi} + 2\zeta\omega_0\,\dot{\phi} + \omega_0^2\left[1 - h\cos(\omega_e t)\right]\phi - \\ - c_3\,\omega_0^2\,\phi^3 - c_5\,\omega_0^2\,\phi^5 = 0 \tag{1}$$

h is the scaled GM fluctuation, defined as $h = \dfrac{GM_{\max} - GM_{\min}}{2\,\overline{GM}}$. In the ABS (2004) guide the corresponding equation becomes identical to (1), if $\overline{GM}$ is interpreted as $\dfrac{GM_{\max} + GM_{\min}}{2}$ and the 5ᵗʰ-order restoring term is omitted. ITTC's boundary of instability (h threshold) refers to infinitesimal perturbations of the upright state, therefore nonlinear restoring terms do not participate. The proposed expression for the first region (principal resonance) is:

$$h = \sqrt{\left(2 - \frac{\omega_e^2}{2\,\omega_0^2}\right)^2 + 4 \cdot \zeta^2 \frac{\omega_e^2}{\omega_0^2}} \qquad (2)$$

This is the 1ˢᵗ-order approximation of the Mathieu functions that truly describe the boundary.

Whilst the generation of instability on this boundary is in reality a 'linear' phenomenon, the finite roll amplitude that accrues from the loss of stability is critically influenced by nonlinearities. Prediction formulae of steady parametric rolling appear in the ITTC guideline, deduced by the method of harmonic balance (Spyrou 2005):

$$c_5 = 0: \quad A^2 = \frac{4}{3\,c_3}\left[\left(1 - \frac{1}{a}\right) \mp \sqrt{\frac{h^2}{4} - \frac{4\zeta^2}{a}}\right] \qquad (3)$$

$$c_5 \neq 0:$$

$$A^2 = -\frac{3c_3}{5c_5} \pm \sqrt{\left(\frac{3c_3}{5c_5}\right)^2 - \frac{8}{5c_5}\left(-1 + \frac{1}{a} \pm \sqrt{\frac{h^2}{4} - \frac{4\zeta^2}{a}}\right)} \qquad (4)$$

where $a = 4\omega_0^2 / \omega_e^2$. The $\mp$ sign reflects the possibility of several stable and unstable states coexisting for the same value of a. After conversion to common symbols, the ABS expression (derived by the method of multiple scales) is identical to (3). There is one logistic difference however: a should be calculated not for the natural frequency ω_a, but for one that is based on the mean metacentric height.

In Fig. 1 is drawn the boundary of principal resonance according to eq. (2). Parameter values that correspond to a post-panamax containership have been used: $\zeta = 0.061275$ at $\omega_0 = 0.2076$ s⁻¹ and a restoring that is initially hardening ($c_3 = -0.99861$). Moreover, an extra boundary curve was drawn, defined according to the following expression (Spyrou 2005):

$$h = \frac{4\zeta}{\sqrt{a}}, \quad a \leq 1 \qquad (5)$$

This new boundary is worthy of special attention, because it is located in the region that is presumed to be characterised by global stability. It is recalled that, whilst the parametric oscillations originate from the boundary of stability of the upright equilibrium state, they are not confined by it but they expand also to its exterior. In particular, those that are subcritically generated, produce a fold bifurcation. For a hardening system these oscillations are initially unstable and they emanate from the left segment of the stability boundary of the linear system. The locus of the fold represents in fact the true (nonlinear) lower boundary of parametric oscillations. Underneath it, no roll oscillation can arise. Despite the complexity of phenomena, the locus of this fold can be determined by equation (5). It becomes thus apparent that the domain of parametric oscillations is broader and, to be correctly specified, eq. (2) should be combined with eq. (5).
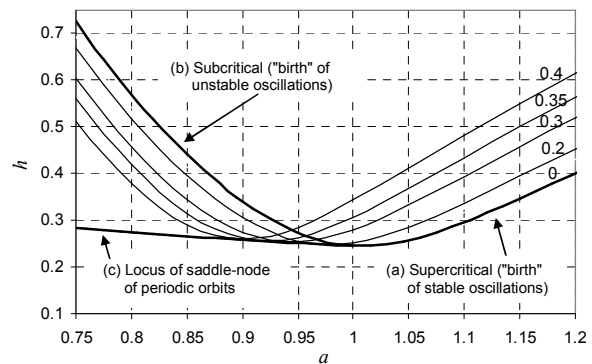
Fig. 1: Main parametric roll boundaries at principal resonance. Iso-lines of constant steady amplitude are shown extending outside the customary boundary.

For each (h, a) pair that falls to the interior of the region defined by the curves (b) and (c) of Fig. 1, two stable states of ship operation coexist: the trivial upright equilibrium 'competes' with at least one stable oscillatory parametric response. As matter of fact, an unsafe transition from the stationary upright state towards the oscillatory one could be realised. Some consolation is offered however by the fact that, such a change of state could come about only discontinuously and thus the presence of some strong perturbation is essential for kicking the system out of its safe basin, provoked e.g. by a strong wind gust. This coexistence, which had been hitherto neglected, means also that parametric oscillations might arise for a wide range of frequency ratios.

THE CONTAINERSHIP

To evaluate the above formulae and also perform further investigations, a post-panamax containership with length 288.87 m was modelled. Rendered view of her wetted area is shown in Fig. 2, obtained with MaxSurf (2006). A glimpse into the variation of *GZ* experienced in waves is seen in Fig. 3.
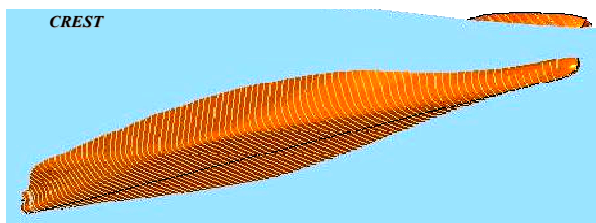

Fig. 2: Characteristic variation of wetted surface of containership between a trough and a crest of a wave.

EVALUATION OF MATHIEU-TYPE SYSTEM THROUGH CONTINUATION

Continuation algorithms usually accept the mathematical model in the autonomous canonical form:

$$\frac{d\mathbf{x}}{dt} = \mathbf{f}(\mathbf{x}; \mathbf{b}) \qquad (6)$$

where $\mathbf{x}$, $\mathbf{b}$ are respectively the state and control parameters' vectors. Variation of one or more elements of the control vector $\mathbf{b}$ creates, through solution of the above vector differential equation, branches of steady-state (in our case periodic) responses. These branches constitute the "spine" of dynamical response of a system and, depending on nonlinearity, they can associate with quite complex manifestations of system dynamics. It is thus imperative to have capability to trace branches of steady-states efficiently. For such a task continuation, a collection of numerical techniques, is indispensable. For mathematical details one may consult Dhooge et al. (2003).
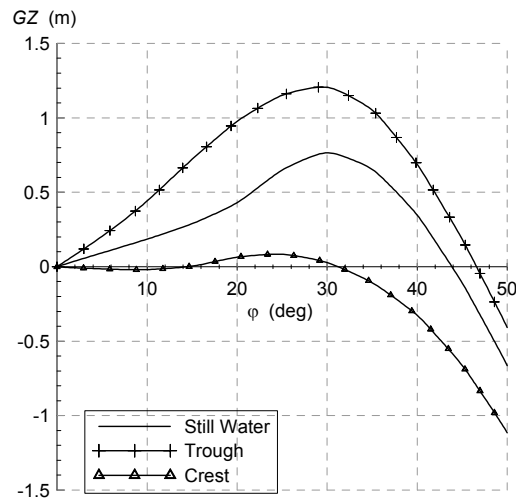

Fig. 3: GZ variation between crest and trough of harmonic wave with λ/L=1.5 and H/λ=1/35.

The basic mathematical model expressed through eq. (1) is characterised by explicit time-dependence in the restoring term. Thus it is not in the autonomous form of eq. (6) obliged by the continuation algorithm. To overcome this, a suitable additional pair of differential equations is introduced whose stable steady states are cyclic: $x = \sin(\omega_e t)$, $y = \cos(\omega_e t)$. Thereafter, eq. (1) is converted into a system of four 1ˢᵗ-order o.d.e.

that, while equivalent to eq. (1), shows no explicit time-dependence.

Branches of steady periodic solutions and the boundary line of parametric rolling were subsequently traced automatically with respect to the following control parameters: the intensity of *GM* variation h ; the frequency parameter a (it is interpreted as $\dfrac{4\omega_0^2}{\omega_e^2}$ if the continuation is used for evaluating the relevant ITTC formula; or as $\dfrac{4\bar{\omega}_a^2}{\omega_e^2}$ when the comparison is against that of ABS. While ω_0 is a function of ship alone, $\bar{\omega}_a$ is affected by the wave); the stiffness parameters c_3, c_5 ; the roll damping ratio ζ .

To systematise comparisons, linear, cubic and quintic fits were developed, each with a specific range of validity in terms of roll angle. Their coefficients, identified by the least-squares method, are shown in Table 1, together with characterisations of these fits.

The dependence of the steady oscillation upon the parametric variation *h* is shown in Figures 4 to 6. Several values of the frequency parameter *a* around principal resonance have been tried. These reveal that the analytical expressions are very suitable for predicting the amplitude of oscillation of the Mathieu-type system (8), even for moderate-to-large *h* (the amplitude is slightly over-predicted).

Continuation was carried out also with the quintic term of the restoring retained. This extra term enables an additional folding of the curve of steady roll amplitude. It is notable that, despite the consideration of large amplitudes where one might expect an analytical perturbation-like approach to fail, the corresponding analytical and numerical curves are kept sufficiently close to each other.

Two-parameter continuation (with respect to h, a) was also performed for capturing directly the boundary of roll oscillations (Fig. 7). The obtained curves have been then contrasted

against the curves derived as plots of the analytical formulae (2) and (5). One notes good degree of coincidence between the two types.

Table 1 : Coefficients of GZ fits.

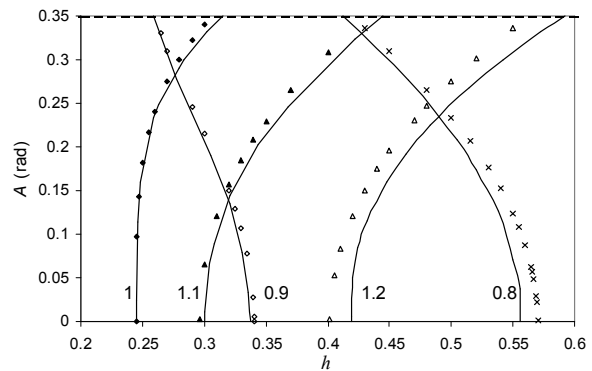|	c_3	c_5	range of validity	quality of fit
linear	-	-	15^0	excellent
cubic hardening	- 0.999	-	20^0	excellent
cubic softening	1.570	-	44^0	weak
quintic hardening	0.484	-12.988	25^0	excellent
quintic softening	- 3.120	8.288	44^0	fair

Fig. 4: Comparison of analytical (dotted) and numerical (continuous line) parametric roll amplitudes for the defined range of validity of the cubic hardening fit.
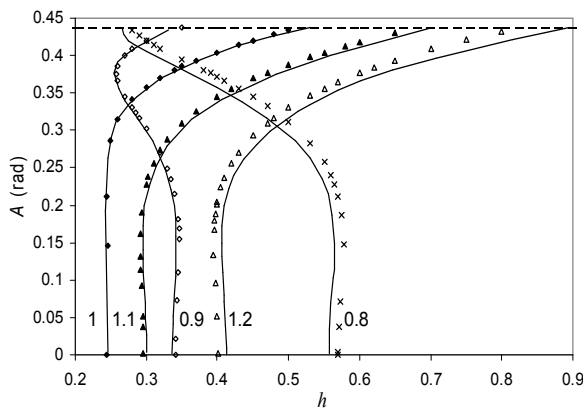
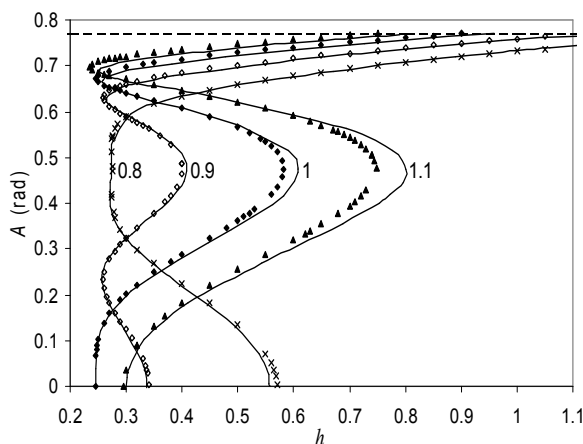Fig. 5: As above, for quintic hardening fit.

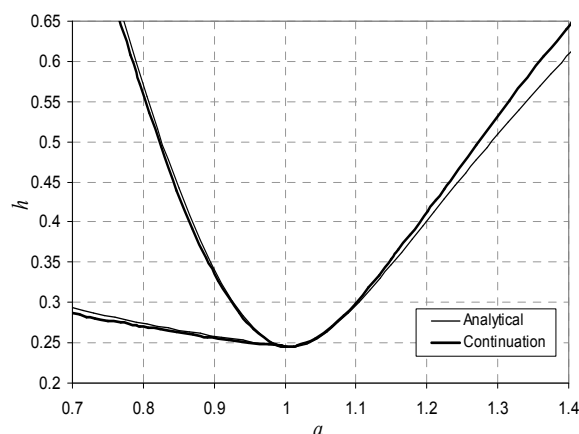Fig. 6: As above, for quintic softening fit.

Fig. 7: Comparison of instability boundaries for a simple Mathieu type model, obtained by analytical formulae and by continuation.

VALIDATION FOR NON-HARMONICALLY VARYING $GZ(\phi,t;H,\lambda)$

The variation of GZ might not be truly symmetric, even in an idealised harmonic wave. Moreover, maximum and minimum GZ values may not be realised exactly at the trough and the crest, respectively. Such features have been met also in the modelled containership. In Fig. 8 is shown a comparison of the calculated fluctuating GM on a harmonic wave with: i) a presumed as harmonically varying GM that presents same level peaks with the original one but zero phase relatively to the wave; ii) the previous harmonic GM with its phase shifted as of the original one. As the differences are prevalent, one wonders how important could these be for the prediction of parametric roll tendency? Thus a further continuation study was undertaken using this time the following roll equation:

$$\ddot{\phi} + 2\zeta\omega_0\,\dot{\phi} + \frac{mg}{J_{XX}}GZ\left(\phi,\omega_e t;H\right) = 0 \qquad (7)$$

'Exact' GZ curves were calculated in advance using MaxSurf, for several positions of the ship on a harmonic wave, in condition of vertical equilibrium. The procedure was repeated for a few combinations of wave length and wave steepness. A 3-parameter fitting procedure was then developed (Scanferla 2006). A snapshot of the result is shown in Fig. 9.

In the first instance, the wave length was fixed to one and a half times the ship length. Values for the coefficients of the GZ function were determined by minimising a merit function defined by the sum of distances squared, measured from the actual data points to the sought nonlinear regression line. In this process preferences may be set: here it was ensured that the GM value obtained from the fit (at some arbitrary longitudinal position on the wave), is practically the same with the true local GM. Concurrence of GM means that no serious difference should be expected in the frequency of encounter where parametric rolling arises.
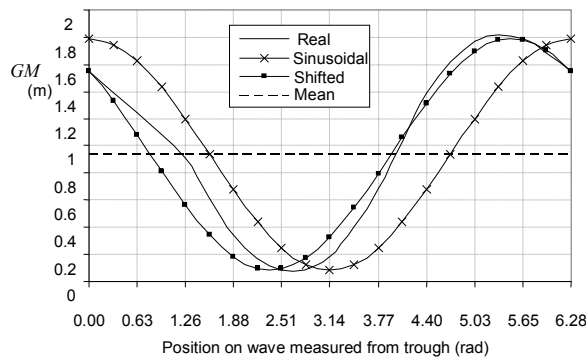
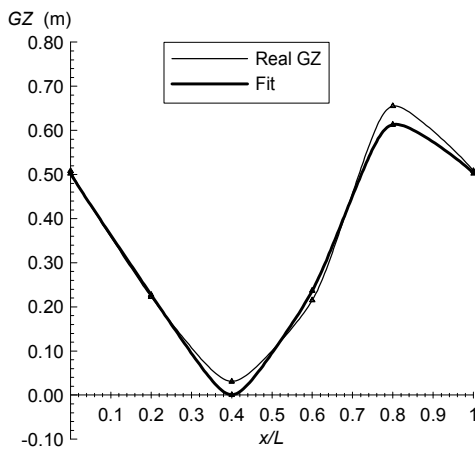**Fig. 8: GM variations for one wave length: λ/L =1.5, H/λ =1/50.**

With the fluctuating *GZ* parameterized with respect to wave height by means of the above fitting process, continuation analysis was subsequently performed. Results were then compared against the analytical ones. It is essential to commend here about the correspondence between the wave height *H* that appears explicitly in eq. (7) and the parametric amplitude *h* that appears in eq. (1). As indicated by Fig. 9, the function $h = f(H)$ becomes nonlinear (softening) at extreme wave heights.

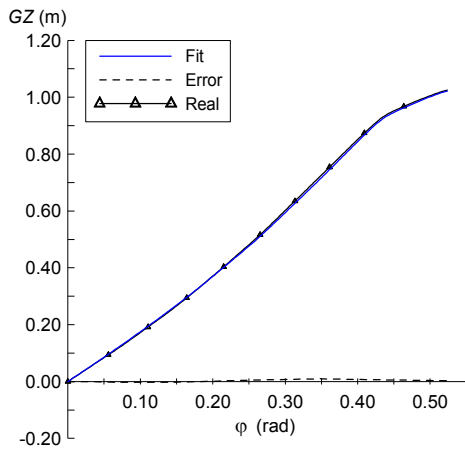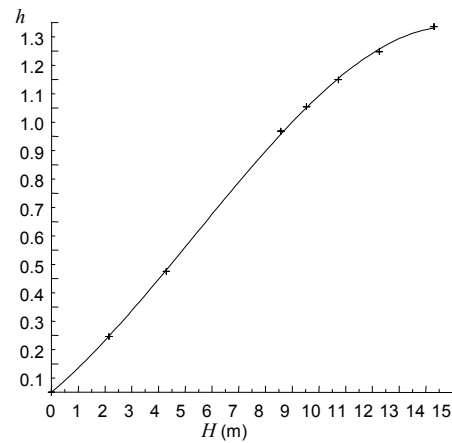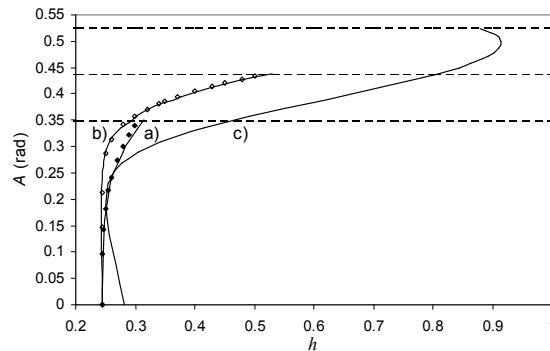**Fig. 10: Relation of wave height with amplitude of parametric excitation.**

Fig. 9: Some indication about the attained quality of GZ fitting for λ/L **=1.5 and** H **= 10.725m: GZ at wave trough (upper); GZ variation along the wave at** $\phi = 0.26$ **rad (lower).**

Fig. 11: Steady parametric amplitudes for a = 1: a) cubic hardening *GZ*, b) quintic hardening, c) Fourier. *Horizontal lines indicate ranges of validity of approximations (*dots for the analytical and continuous lines for the numerical).
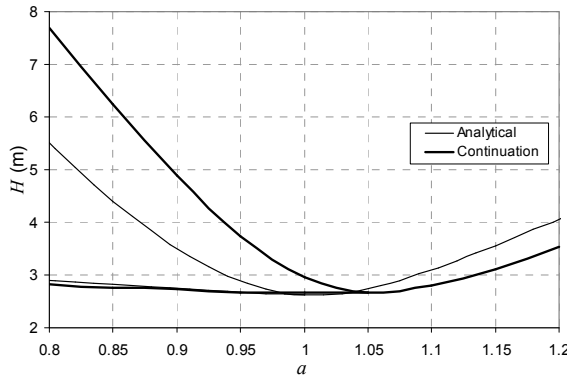
Fig. 12: Comparison of boundaries of instability obtained by use of the analytical formulae and by the "Fourier *GZ*".

The effect owed to the more accurate representation of the *GZ* function is considerable (Fig. 11). More illuminating is a comparison concerning the boundary of parametric rolling on the (*a*, *H*) parameters' plane, revealing the following characteristic (Fig. 12): the new boundary line seems to be shifted in comparison to the one obtained from the simpler Mathieu-type model. This is interpreted as being due to the non-symmetric variation of *GM* and the fact that the mean *GM* value departs from the one of harmonic variation.

IMPLEMENTATION OF A HEAVE-PITCH-ROLL MODEL

At this stage a different direction was followed and a coupled roll-pitch-heave model was implemented (Gavriilidis 2007). By this could be taken into account the effect that one expects to be introduced by vertical plane dynamics, related to the fact that the principal resonance appears at an encounter frequency that is not particularly low. The mathematical model used was very similar to the one published by Neves & Rodriguez (1996) and is given briefly here in standard notation. The hydrodynamic coefficients as well as direct excitations (Froude-Krylov) were calculated from the strip method of Maxsurf's Seakeeper code taking as basis frequency the condition of principal resonance. Hydrostatic coefficients were calculated analytically. The coefficients

that were extra to those that have appeared previously and a non-zero value was appropriate or was eventually used for them, are found in Table 2. The derivatives due to wave passage were calculated internally (in fact these produce the parametric excitation) because they are time dependant; e.g. for

$Z_{\zeta z}(t) = 2\rho g \int_L \frac{\partial \overline{y}}{\partial z} \zeta \, dx$ the following steps are

taken: the wave profile $\zeta = \overline{\zeta} \cos k(x - ct)$ at each section is determined. The result of the

above calculation is multiplied by $\left(\frac{\partial \overline{y}}{\partial \overline{z}}\right)$ for

each section. Finally, "per section" results were calculated along the ship length.

$$\left(m + Z_{\ddot{z}}\right) \cdot \ddot{z} + Z_{\dot{z}} \cdot \dot{z} + Z_{\ddot{\theta}} \cdot \ddot{\theta} + Z_{\dot{\theta}} \cdot \dot{\theta} + + Z_z \cdot z + Z_\theta \cdot \theta +$$

$$+ \frac{1}{2} Z_{zz} \cdot z^2 + \frac{1}{2} Z_{\phi\phi} \cdot \phi^2 + \frac{1}{2} Z_{\theta\theta} \cdot \theta^2 + Z_{z\theta} \cdot z\theta +$$

$$+ \frac{1}{2} Z_{\phi\phi z} \cdot \phi^2 \cdot z + \frac{1}{2} Z_{\phi\phi\theta} \cdot \phi^2 \cdot \theta + Z_{\zeta z}(t) \cdot z + Z_{\zeta\theta}(t) \cdot \theta +$$

$$+ Z_{\zeta zz}(t) \cdot z^2 + Z_{\zeta z\theta}(t) \cdot z\theta + Z_{\zeta\phi\phi}(t) \cdot \phi^2 = Z_w(t)$$

$$\left(I_{xx} + K_{\ddot{\phi}}\right) \cdot \ddot{\phi} + K_{\dot{\phi}} \cdot \dot{\phi} + K_\phi \cdot \phi + K_{z\phi} \cdot z\phi$$

$$+ K_{\theta\phi} \cdot \theta\phi + \frac{1}{2} K_{zz\phi} \cdot z^2\phi + \frac{1}{2} K_{\theta\theta\phi} \cdot \theta^2\phi$$

$$+ \frac{1}{6} K_{\phi\phi\phi} \cdot \phi^3 + K_{z\phi\theta} \cdot z\phi\theta + K_{\zeta\phi}(t) \cdot \phi +$$

$$+ K_{\zeta\zeta\phi}(t) \cdot \phi + K_{\zeta z\phi}(t) \cdot z\phi + K_{\zeta\phi\theta}(t) \cdot \phi\theta = 0$$

$$\left(I_{yy} + M_{\ddot{\theta}}\right) \cdot \ddot{\theta} + M_{\dot{\theta}} \cdot \dot{\theta} + M_{\ddot{z}} \cdot \ddot{z} + M_{\dot{z}} \cdot \dot{z} + M_z \cdot z + M_\theta \cdot \theta +$$

$$+ \frac{1}{2} M_{zz} \cdot z^2 + \frac{1}{2} M_{\phi\phi} \cdot \phi^2 + \frac{1}{2} M_{\theta\theta} \cdot \theta^2 + M_{z\theta} \cdot z\theta$$

$$+ \frac{1}{2} M_{\phi\phi z} \cdot \phi^2 \cdot z + \frac{1}{2} M_{\phi\phi\theta} \cdot \phi^2 \cdot \theta + \frac{1}{2} M_{\theta\theta} \cdot \theta^2 \cdot z + \frac{1}{6} M_{\theta\theta\theta} \cdot \theta^3$$

$$+ M_{\zeta z}(t) \cdot z + M_{\zeta\theta}(t) \cdot \theta + M_{\zeta z\theta}(t) \cdot z\theta + M_{\zeta\phi\phi}(t) \cdot \phi^2 = M_w(t)$$

(8)

Roll amplitudes as functions of wave height are presented in Fig. 13, for frequency ratios

around principal resonance. These curves were produced automatically by continuation which thus have worked successfully for the coupled model too. One observes that, for the coupled model, parametric roll seems easier to be realized. This is in line with similar observation by Neves. The matter certainly needs to be investigated further. It was similarly confirmed that the 2nd order model, i.e. if the 3rd order terms were neglected, does not produce realistic results (response amplitudes were diverging to infinity).
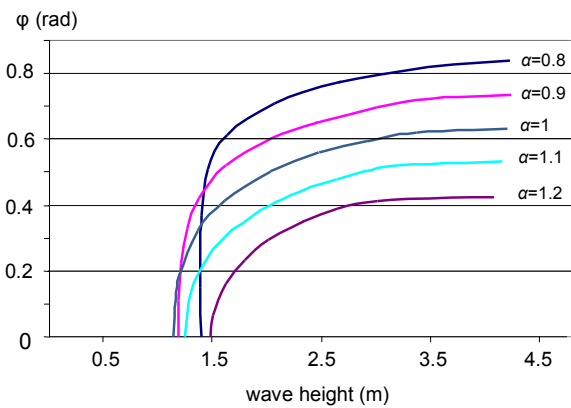

Fig. 13: Parametric roll amplitudes based on coupled model.

CONCLUSIONS

The analytical formulae can successfully characterise the behaviour of a principally Mathieu-type system. However, as the mathematical model incorporates more detail, featuring for example a non-harmonic variation of *GZ* in waves, their quantitative prediction potential of parametric roll is placed in doubt.

It is essential to be recognised that the boundary of parametric oscillations is defined by the locus of the saddle-nodes of the parametric oscillations in combination with the locus of the supercritical birth of parametric oscillations.

Numerical continuation can automate the derivation of parametric rolling boundaries and of steady-state responses. More complex mathematical models may also be accommodated.

The coupled roll-heave-pitch model showed considerably easier inception of parametric rolling, a matter that is worthy further investigation.

Table 2: Coefficients of coupled model.

Inertia	
$m + Z_{\ddot{z}}$ 149,647,024 kg	$I_{yy} + M_{\ddot{\theta}}$ 752,763,959,062 kg m^2
$Z_{\ddot{\theta}}$ 1,810,274,280 kg m	$M_{\ddot{z}}$ 3,706,664,872 kg m
Damping	
$Z_{\dot{z}}$ 72,870,518 kg/s	$M_{\dot{\theta}}$ 380,795,280,003 kg m^2/s
$Z_{\dot{\theta}}$ 1,767,114,533 kg m/s	$M_{\dot{z}}$ 1,074,248,812 kg m/s
Linear hydrostatic	
Z_z 101,698,799 kg/s^2	M_z 1,360,729,924 kg m/s^2
Z_θ 1,360,729,924 kg m/s^2	M_θ 501,777,639,019 kg m^2/s^2
2nd order hydrostatic	
Z_{zz} -2,248,333 kg/(m s^2)	M_{zz} -28,198,195 kg/s^2
$K_{z\phi}$ -572,683,808 kg m/s^2	$Z_{z\theta}$ -28,198,195 kg/s^2
$M_{z\theta}$ -30,727,106,142 kg m/s^2	$Z_{\phi\phi}$ -572,683,809 kg m/s^2
$M_{\phi\phi}$ -35,978,008,003 kg m^2/s^2	$K_{\phi\theta}$ -35,978,008,003 kg m^2/s^2
$Z_{\theta\theta}$ -30,727,106,143 kg m/s^2	$M_{\theta\theta}$ -916,776,984,097 kg m^2/s^2
3rd order hydrostatic	
$Z_{\phi\phi z}$ 198,242,332 kg/s^2	$Z_{\phi\phi\theta}$ 10,191,624,112 kg m/s^2
$K_{zz\phi}$ 198,242,332 kg/s^2	$K_{\theta\theta\phi}$ 2,060,120,263,668 kg m^2/s^2
$M_{\phi\phi z}$ 10,191,624,112 kg m/s^2	$M_{\phi\phi\theta}$ 2,060,120,263,668 kg m^2/s^2
$M_{\theta\theta\theta}$ 1,040,935,897,781 kg m^2/s^2	$K_{z\phi\theta}$ 10,191,624,111 kg m/s^2

REFERENCES

ABS, 2004 ABS *Guide for the Assessment of Parametric Roll Resonance in the Design of Container Carriers*, American Bureau of Shipping.

Dhooge A., Govaerts W., Kuznetsov Yu.A., Mestrom W., Riet A.M. and Sautois B. 2003: *MATCONT* and *CL_MATCONT: Continuation Toolboxes for MATLAB*. Report of Gent (Belgium) and Utrecht (Netherlands) Universities.

Gavriilidis, A. (2007) Development of a 3DOF model for the simulation of the parametric rolling motion of a containership. Diploma Thesis, National Technical University of Athens.

MaxSurf 2006, Formation Design Systems, User Manual.

ITTC 2004, *Predicting the Occurrence and Magnitude of Parametric Rolling*, Guideline 7.5-02-07-04.3, 7 pages.

Neves, M.A.S. (ed.) 2006, *Proceedings*, 9th International Conference on Stability of Ships and Ocean Vehicles, Rio de Janeiro, October.

Neves, M.A.S. & Rodriguez, C.A. 2006 An investigation on roll parametric resonance in regular waves. *Proceedings*, 9th International Conference on Stability of Ships and Ocean Vehicles, 99-108.

Scanferla, G. 2006 Development of a computational procedure for the derivation of boundaries of parametric roll in a longitudinal seaway. Diploma Thesis. Erasmus/Socrates exchange from the University of Trieste to the National Technical University of Athens.

Spyrou, K.J. 2005 Design criteria for parametric rolling. *Oceanic Engineering International*, ECOR, **9**, 1, 11-27.